

Comparison of different optical coherence tomography devices for diagnosis of non-melanoma skin cancer

S. Schuh¹, R. Kaestle¹, E. Sattler^{2,#} and J. Welzel^{1,#}

¹Department of Dermatology and Allergology, General Hospital Augsburg, Augsburg, Germany and ²Department of Dermatology and Allergology, Ludwig-Maximilian University of Munich, Munich, Germany

Purpose: To compare the diagnostic imaging ability of three different optical coherence tomography (OCT) devices in non-melanoma skin cancer (NMSC).

Methods: Thirty actinic keratoses (AKs) and 27 basal cell carcinomas (BCCs) of 29 patients were examined with three different OCT devices, VivoSight[®], Callisto[®] and Skintell[®].

Results: Complete data sets were available for 16 BCCs and 10 AKs of 18 patients. All OCT devices were able to discriminate BCCs and AKs significantly from perilesional normal skin due to lower signal intensities as well as a thicker stratum corneum and epidermis in AKs. A significant decrease in the signal intensity and thickness of all skin layers was noted with Skintell[®] in contrast to VivoSight[®] and Callisto[®]. OCT comparisons revealed only slight differences between VivoSight[®] and Callisto[®]. Regarding BCC tumor thickness VivoSight[®] and Callisto[®] correlated well, histology did not correlate with the three

OCT devices, whereas Skintell[®] showed no correlation with VivoSight[®], Callisto[®] or histology.

Conclusion: All tested OCT devices could identify BCCs and AKs objectively through standardized measurement of signal intensity and skin layer thickness. Due to their technical specifications (resolution, penetration depth), each of the OCT systems offers additional and special information on NMSC.

Key words: optical coherence tomography – non-melanoma skin cancer – basal cell carcinoma – actinic keratosis – skin imaging – OCT devices

OPTICAL COHERENCE tomography (OCT) is an optical imaging method for the *in vivo* display of tissue, which was first described by Fercher et al. (1) and Huang et al. (2) in ophthalmology. With its high resolution of 3–15 µm due to the broadband light source and its penetration depth of 1–2 mm, depending on the scattering and absorption features of the light beam, the OCT provides a non-invasive cross-sectional view on superficial skin layers (3).

Through typical morphological characteristics, basal cell carcinomas (BCCs) and actinic keratoses (AKs) can be diagnosed in OCT. Both AKs and BCCs have no regular skin layer arrangement and in AKs a thicker stratum corneum and epidermis is found (4, 5). AKs present with hyporeflexive streaks, bright bands and flakes in the stratum corneum and epidermis (5, 6). BCCs look like signal-poor ovoid nodules with a dark rim in a hyper reflective

fibrous stroma (7). Despite the structural criteria, AKs, BCCs and their differential diagnoses are still difficult to distinguish and therefore more studies like the one by Gao et al. on quantitative objective parameters like signal intensity are needed (8, 9). Many of the investigations on non-melanoma skin cancer (NMSC) morphology were conducted with only one of the OCT devices VivoSight[®], Callisto[®] or Skintell[®], but a comparison of the devices is still lacking (3, 10–13).

Hence, the aim of this study was to compare three different OCT devices regarding their diagnostic imaging ability of NMSC such as signal intensity and thickness measurements and, where possible, in comparison with histology.

Materials and Methods

Patients and study performance

Patients aged over 18 years, good quality OCT images, unequivocal clinically and

[#]Both authors act as senior authors.

dermoscopically diagnosed AKs/BCCs and unimpaired perilesional normal skin as a control location, were included in the study. After acquiring written informed consent, the patients were examined clinically and dermoscopically by a dermatologist and the preliminary diagnosis was established. Affected skin lesions were photographed with a Panasonic Lumix DMC-TZ8 and were scanned with three different OCT devices (VivoSight[®], Callisto[®], Skintell[®]) before therapy. If the lesion was larger than the measurable area of each OCT device, the measurement was taken in the center.

Fifty-seven lesions (30 AKs and 27 BCCs) of 29 patients (7 female, 22 male, median age 71.3, range 53–95 years) were included in this experimental study. The NMSC affected mainly the head and neck region (24 AKs, 14 BCCs), the trunk (3 AKs, 12 BCCs) and arm (3 AKs, 1 BCC).

Because of the location of some lesions (e.g. the external ear or the inner eye corner), the imaging of six AKs examined by Skintell[®] as well as of two BCCs and four AKs investigated by Callisto[®], was not possible. Due to poor image quality, the images of nine BCCs and of two AKs measured by Callisto[®], as well as of eight AKs taken by Skintell[®], were excluded. Complete data sets with measurements of all three OCT devices were available for evaluation of 26 lesions (16 BCCs and 10 AKs) of 18 patients (3 female, 15 male, median age 72.1, range 53–85 years).

The measurements were performed from September 2011 to March 2014 at the Department of Dermatology and Allergology of the General Hospital in Augsburg.

The protocol was approved by the Ethical Committee of the Ludwig-Maximilian University (Project number 221-11) and by the ethic vote of the University of Lübeck in 1997. The study was conducted according to the principles of the declaration of Helsinki and international guidelines concerning human studies.

Optical coherence tomography devices

Examinations were performed with three different OCT devices: a swept-source multi beam frequency domain OCT, a spectral domain (SD) OCT and a time domain high-definition (HD) OCT.

The frequency domain OCT device VivoSight[®] (Michelson Diagnostics, Kent, UK) offers a lateral optical resolution of $<7.5 \mu\text{m}$ and an axial resolution of $10 \mu\text{m}$. The penetration depth lies at about 1.5–2 mm due to scattering effects (14). Using the multi-slice function, VivoSight[®] reaches a three-dimensional scanning range of $6 \text{ mm} \times 6 \text{ mm} \times 2 \text{ mm}$ and is a swept-source multi beam frequency domain OCT system. The light source is a special laser based on Michelson interferometry (HSL 2000; Santec Corporation, Komaki, Japan) with a wavelength of 1305 nm (14).

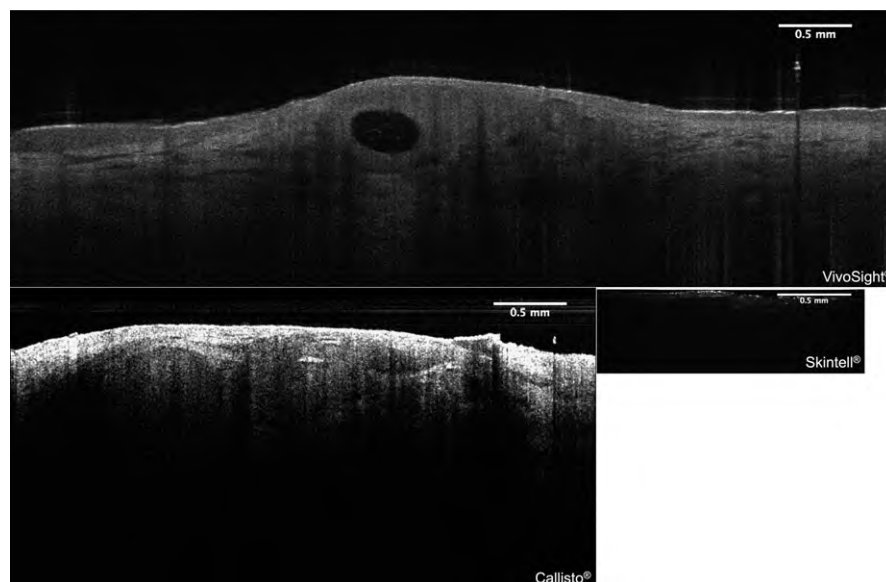


Fig. 1. BCC measured with all three OCT systems VivoSight[®], Callisto[®] and Skintell[®].

The second tested OCT device is the SD-OCT system Callisto[®] (Thorlabs AG, Lübeck, Germany), which has a detection depth of 1.7 mm from the skin surface (15). It has an axial resolution <math><7\ \mu\text{m}</math> and a lateral resolution of about 8 μm with a lateral scan length of up to 10 mm, providing cross-sectional images (15).

This frequency domain OCT system contains a 930 nm super luminescent diode light source with a broadband, lower coherence light (15).

The third used OCT device is Skintell[®] (AGFA HealthCare, Mortsel, Belgium), a time domain HD-OCT system, which is able to take 2D-images with a field of view of 1.8 mm \times 1.5 mm

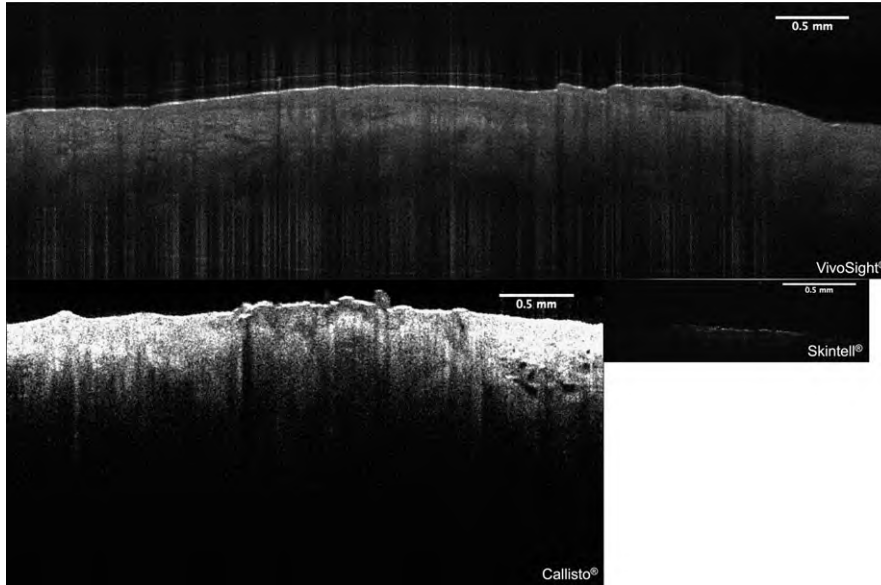
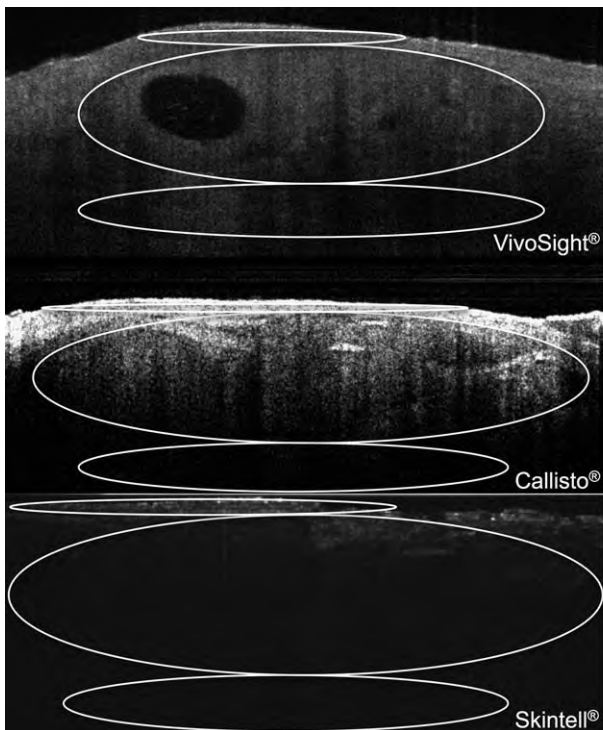


Fig. 2. AK measured with all three OCT devices VivoSight[®], Callisto[®] and Skintell[®].



Signal intensity of BCCs compared to perilesional normal skin by three OCT devices

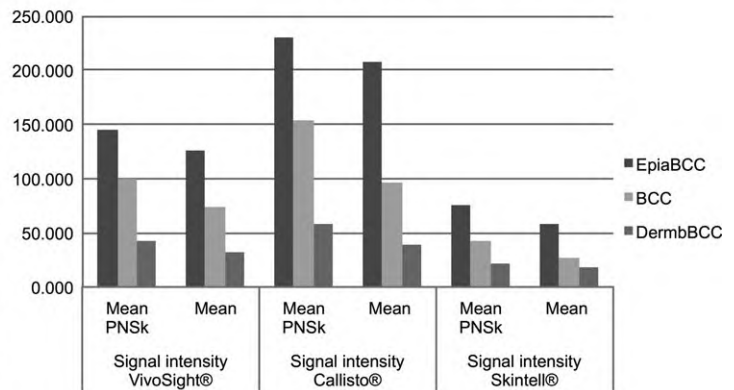


Fig. 3. Signal intensity of BCCs compared to adjacent normal skin visualized by three OCT systems; signal intensity in grayscale (0 = black, 255 = white).

and a penetration depth of about 750 μm (16). There is the possibility of capturing both cross-sectional (slice) and horizontal (en face) images in real time as well as 3D images (16). This OCT system offers a high axial and lateral resolution of 3 μm and works in the near infrared range at about 1000–1700 nm (16). The application of an optical matching gel (Skintell[®] optical gel; AGFA HealthCare) between the glass plate of the hand piece and the skin surface is necessary for the measurement (16).

Image analysis

The saved sequences of OCT images taken *in vivo* were reviewed and representative single images were chosen for evaluation. In order not to influence the signal intensity measurements, the unprocessed images were analyzed with Image J.

Through the use of the polygon tool and the function for histogram analysis, the signal intensity was calculated. The histogram shows a frequency distribution of the gray levels, which are plotted on the *x*-axis from 0 (black) to 255 (white), in the image. The determined average gray level yields the signal intensity, which was used for the comparisons in the statistical analysis.

Stratum corneum and epidermis thickness of AKs, as well as thickness measurements of tumor and epidermis above the BCCs in the OCT image and in histology, were conducted from the top of the skin surface down to the BCC/AK border. In healthy skin, the stratum corneum can often be found as a small layer below the hyper reflective band. The epidermis, however, ranges from the bright skin surface reflection down to the first visible dark small band, which is the dermal-epidermal junction.

Statistical analysis

For the collection of data, Microsoft Office Excel for Mac 2011 was used. The statistical analysis was performed using IBM SPSS Statistics software for Mac (SPSS 21.0; IBM Corp., Armonk, NY, USA). All the data of each group underwent normality tests (like Kolmogorov–Smirnov Test or modified by Lilliefors) to look for normal distribution. With a normal distribution, paired sample *t*-tests were used for intra-individual comparisons of BCCs/AKs and

TABLE 1. Statistical analysis of the comparison of three OCT devices regarding (a) BCCs and AKs in comparison to perilesional normal skin and (b) concerning the skin layer thickness in AKs compared to healthy skin

(a)	Signal intensity VivoSight [®]				Signal intensity Callisto [®]				Signal intensity Skintell [®]				P-value	
	Mean	PNSk	SD	P-value	Mean	PNSk	SD	P-value	Mean	PNSk	SD	P-value		
AK														
Sc	212.4	129.2	15.1	26.9	0.005	231.5	179.3	41.4	0.005	123.8	60.2	47.2	22.3	0.005
Epi	153.4	104.9	8.9	22.5	0.005	204.4	146.1	42.5	0.005	71.0	42.8	26.9	15.5	0.005
Derm	61.6	35.8	9.3	10.2	0.005	81.0	54.6	24.7	0.005	25.8	18.7	8.9	5.8	0.005
BCC														
Epi	144.4	126.7	17.9	21.1	0.002	230.2	207.3	33.5	0.002	75.4	58.4	33.9	23.8	0.002
BCC	99.1	73.0	19.9	19.6	0.001	153.6	96.9	50.8	0.001	42.3	26.8	20.6	9.8	0.002
Derm	42.7	32.8	15.2	15.0	0.001	58.6	39.0	27.5	0.002	21.6	18.7	8.1	6.8	0.001
(b)	Thickness VivoSight [®]				Thickness Callisto [®]				Thickness Skintell [®]					
AK														
Sc	0.015	0.229	0.006	0.177	0.005	0.019	0.221	0.136	0.005	0.016	0.110	0.006	0.060	0.005
Epi	0.092	0.460	0.017	0.299	0.005	0.112	0.440	0.177	0.005	0.074	0.205	0.019	0.067	0.005

PNSk, perilesional normal skin; Epi, epidermis above BCC; Derm, dermis; SD, standard deviation; signal intensity in gray-scale (0 = black, 255 = white), thickness in mm, P-value in bold letters.

perilesional normal skin. If there was no normal distribution within the data or if there was only a small number of samples, Wilcoxon tests for matched pairs were done instead. All three OCT groups were analyzed using Friedman tests. In case of significance, Wilcoxon tests and subsequent Bonferroni-adjustment of *P*-values were performed. For the OCT - histology correlation, Spearman's correlation coefficients were calculated. A *P*-value <0.05 was considered as statistically significant.

Results

The images of BCCs and AKs taken by the three OCT devices (VivoSight®, Callisto® and Skintell®) differ distinctly from each other with regard to image detail, resolution and penetration depth of the signal (see Figs 1 and 2). VivoSight® provides the largest overview with 6 mm × 2 mm, followed by Callisto® with 4 mm × 2 mm and Skintell® with 1.8 mm × 1 mm. VivoSight® also has the highest penetration depth, which is, however, very comparable

to Callisto®, which provides brighter but more granular appearing images. Moreover Skintell® offers the best resolution, but with a clearly smaller picture detail.

Signal intensity of BCCs and AKs as well as skin layer thickness of AKs in contrast to adjacent normal skin visualized by three OCT devices

With every OCT device the mean signal intensity of the BCC, the epidermis above the BCC, as well as of the dermis beneath the BCC, was measured in comparison to the adjacent normal skin layer. In BCC, lower local signal intensities in affected skin layers compared to perilesional healthy skin can be detected (Fig. 3).

All OCT devices show a significant difference between the mean signal intensity of the epidermis above the BCC, of the BCC itself just as of beneath the BCC and healthy surrounding skin layers. Correlating *P*-values are given in Table 1a.

In AKs the mean thickness and signal intensity of the stratum corneum and of the

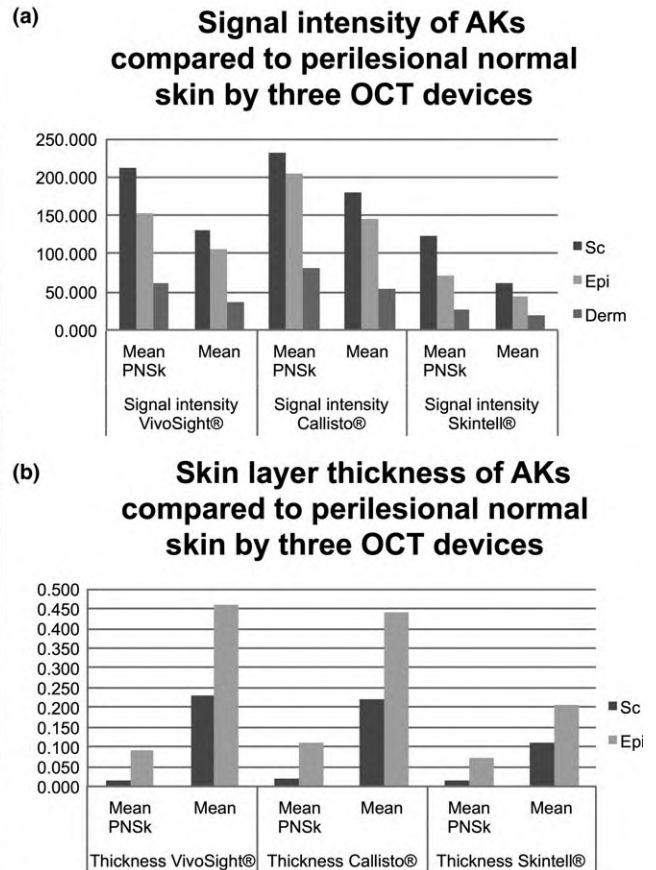
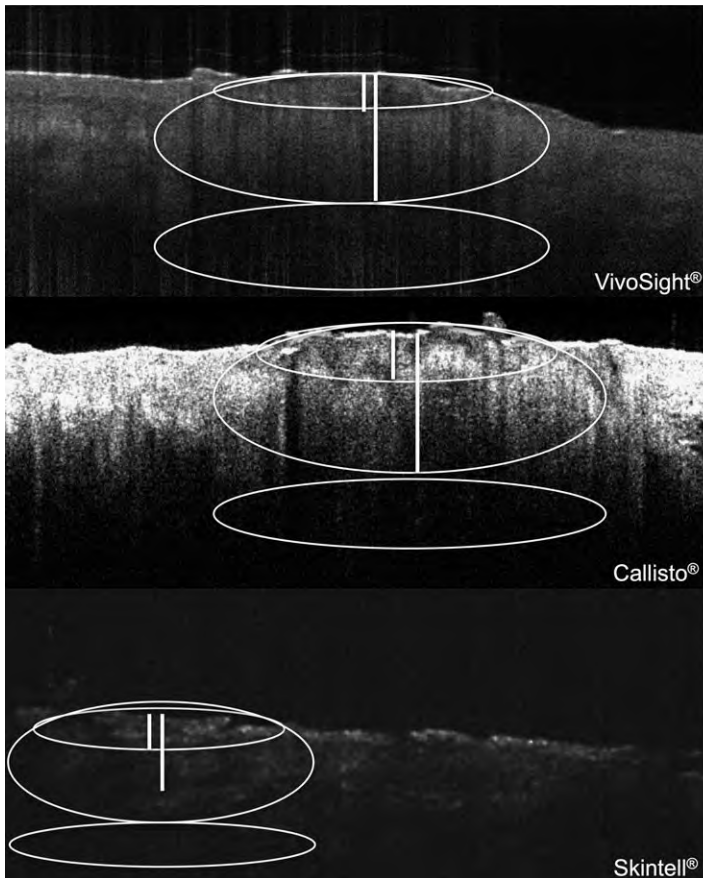


Fig. 4. (a) Signal intensity and (b) skin layer thickness of AKs compared to healthy skin visualized by three OCT devices; thickness in mm, signal intensity in grayscale (0 = black, 255 = white).

epidermis, as well as the signal intensity of the dermis in contrast to perilesional normal skin, were determined in the images of all three OCT devices. A decrease in the local signal intensity in all affected skin layers in relation to neighboring normal skin is found with every single OCT system (Fig. 4a). A thicker stratum corneum and epidermis in AKs vs. healthy skin can be observed for every OCT device (Fig. 4b). The statistical analysis can be seen in Table 1.

There are significant differences between the thickness of the stratum corneum as well as of the epidermis in AKs and in all three cases of signal intensity measurements of AKs compared to normal skin ($P < 0.0001$ to $P < 0.001$).

Comparison of three OCT devices concerning signal intensity of AKs and BCCs and skin layer thickness of AKs

16 BCCs show a lower mean signal intensity of the epidermis above the BCC, the BCC and the

dermis below the BCC with the OCT system Skintell[®] compared to the other two OCT devices and a higher signal intensity with Callisto[®] in relation to VivoSight[®] (Fig. 5a).

The use of Friedman's test shows that there are statistically significant changes in the signal intensity measurement of BCC afflicted skin layers with the three OCT devices (Table 2a). The results of the application of paired Wilcoxon tests with Bonferroni corrected levels of observed significance can be seen in Table 2a, which demonstrates that with Skintell[®], the signal intensity of all the skin layers affected by the BCC is significantly lower than with VivoSight[®] and Callisto[®] measurements. Despite this, OCT examinations with VivoSight[®] compared to Callisto[®] are not significantly different from each other aside from the differences in the signal intensity of the epidermis above the BCC.

10 AKs were measured with the three OCT systems regarding the mean thickness and signal intensity of the stratum corneum, the

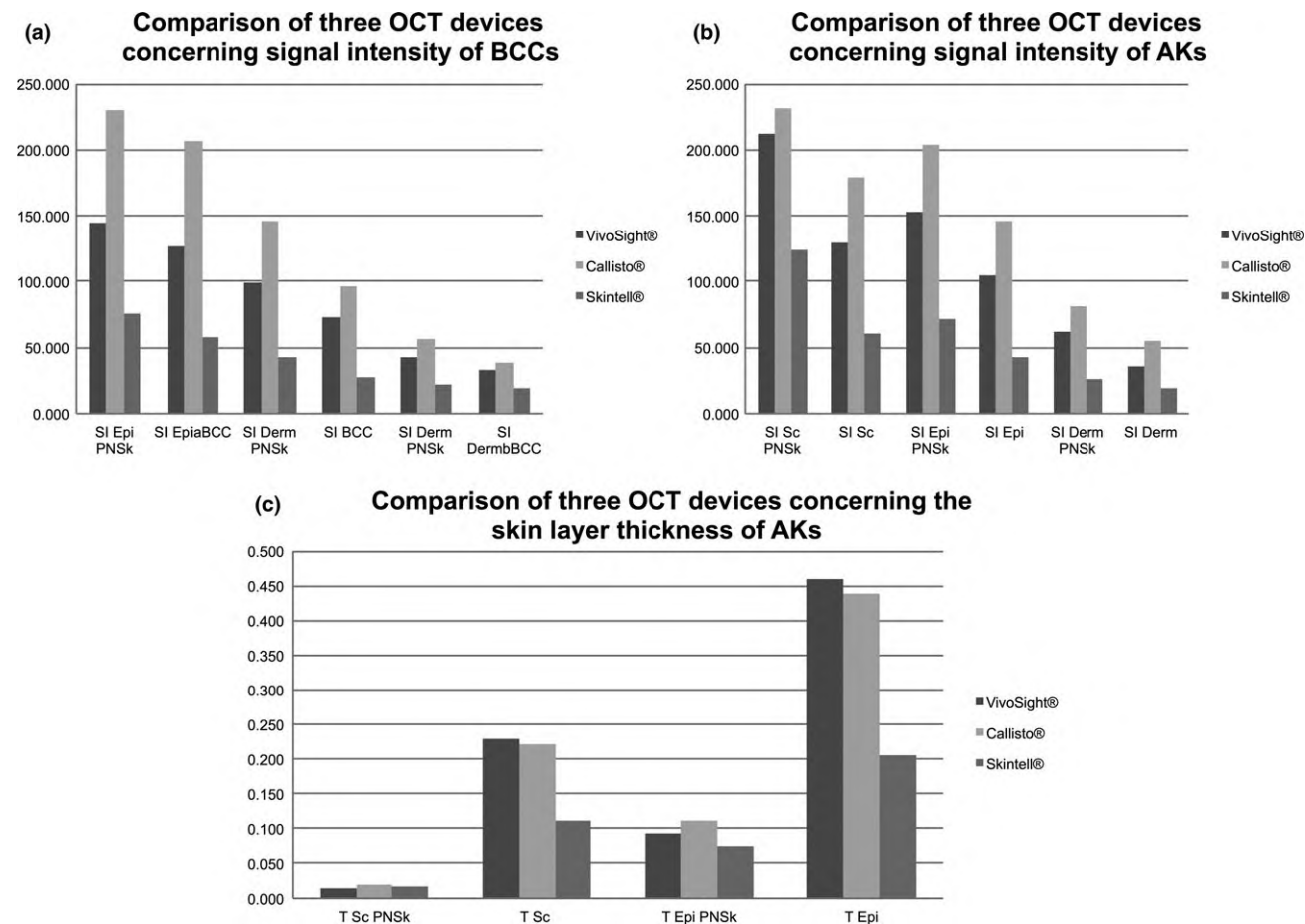


Fig. 5. Comparison of three OCT devices concerning (a) signal intensity of BCCs and (b) AKs and (c) skin layer thickness of AKs; PNSk, perilesional normal skin; EpiBCC, epidermis above BCC; DermBCC, dermis beneath BCC; Sc, stratum corneum; Epi, epidermis; Derm, dermis; T, thickness; SD, standard deviation; signal intensity in greyscale (0 = black, 255 = white), thickness in mm.

TABLE 2. Summary statistics for the comparison of three OCT devices concerning (a) signal intensity of AKs and BCCs and (b) skin layer thickness of AKs

(a)	Friedman's test	Signal intensity VivoSight®-Skintell®				Signal intensity VivoSight®-Callisto®				Signal intensity Callisto®-Skintell®					
		Mean VivoSight®	SD VivoSight®	Mean Skintell®	SD Skintell®	Mean VivoSight®	SD VivoSight®	Mean Callisto®	SD Callisto®	Mean Callisto®	SD Callisto®	Mean Skintell®	SD Skintell®	P-value	
AK															
Sc	$\chi^2 = 18.200$, df = 2, P = 0.0001	129.2	26.9	60.2	22.3	0.015	129.2	179.3	26.9	41.4	0.027	179.3	60.2	22.3	0.015
Epi	$\chi^2 = 18.200$, df = 2, P = 0.0001	104.9	22.5	42.8	15.5	0.015	104.9	146.1	22.5	42.5	0.051	146.1	42.8	15.5	0.015
Derm	$\chi^2 = 15.800$, df = 2, P = 0.0001	35.8	10.2	18.7	5.8	0.015	35.8	54.6	10.2	24.7	0.084	54.6	18.7	5.8	0.015
BCC															
EpiabCC	$\chi^2 = 32.000$, df = 2, P < 0.0001	126.7	21.1	58.4	23.8	0.0012	126.7	207.3	21.1	33.5	0.0012	207.3	58.4	23.8	0.0012
BCC	$\chi^2 = 21.875$, df = 2, P = 0.00002	73.0	19.6	26.8	9.8	0.0012	73.0	96.9	19.6	50.8	0.090	96.9	26.8	9.8	0.003
DermBCC	$\chi^2 = 9.125$, df = 2, P = 0.01	32.8	15.0	18.7	6.8	0.006	32.8	39.0	15.0	22.0	0.702	39.0	18.7	6.8	0.012
(b)															
AK															
Sc	$\chi^2 = 7.400$, df = 2, P = 0.025	0.229	0.177	0.110	0.060	0.039	0.229	0.221	0.177	0.136	1.000	0.221	0.110	0.136	0.021
Epi	$\chi^2 = 13.400$, df = 2, P = 0.001	0.460	0.299	0.205	0.067	0.021	0.460	0.440	0.299	0.177	0.855	0.440	0.205	0.177	0.015

PNSk, perilesional normal skin; EpiabCC, epidermis above BCC; DermBCC, dermis beneath BCC; Sc, stratum corneum; Epi, epidermis; Derm, dermis; SD, standard deviation; signal intensity in gray-scale (0 = black, 255 = white), thickness in mm, P-value in bold letters.

TABLE 3. Statistical analysis of the histologically confirmed 12 BCCs with three OCT systems; (a) Signal intensity of histologically confirmed BCCs in contrast to adjacent normal skin, (b) Comparison of three OCT devices concerning the signal intensity of the BCCs

	Signal intensity VivoSight®				Signal intensity Callisto®				Signal intensity Skintell®							
	Mean	PNSk	SD	P-value	Mean	PNSk	SD	P-value	Mean	PNSk	SD	P-value				
BCC																
EpiaBCC	143.6	120.0	17.1	19.3	226.5	196.2	15.7	31.3	72.1	52.6	33.2	22.9				
BCC	96.7	65.5	17.7	11.0	143.1	76.7	26.9	36.1	41.6	24.6	22.7	8.5				
DermbBCC	44.2	32.4	15.8	16.6	53.8	31.4	29.5	18.5	22.4	19.1	8.4	7.3				
					Signal intensity VivoSight®-Callisto®				Signal intensity Callisto®-Skintell®							
					Mean	PNSk	SD	P-value	Mean	PNSk	SD	P-value	Mean	PNSk	SD	P-value
BCC																
EpiaBCC	$\chi^2 = 24.000$, df = 2, $P < 0.0001$	120.0	52.6	19.3	22.9	120.0	196.2	19.3	31.3	196.2	52.6	31.3	22.9	31.3	22.9	0.006
BCC	$\chi^2 = 15.167$, df = 2, $P = 0.001$	65.5	24.6	11.0	8.5	66.5	76.7	11.0	36.1	76.7	24.6	36.1	8.5	36.1	8.5	0.009
DermbBCC	$\chi^2 = 4.667$, df = 2, $P = 0.097$	32.4	19.1	16.6	7.3	32.4	31.4	16.6	18.5	31.4	19.1	18.5	7.3	18.5	7.3	0.084

PNSk, perilesional normal skin; EpiaBCC, epidermis above BCC; DermbBCC, dermis beneath BCC; SD, standard deviation; signal intensity in grayscale (0 = black, 255 = white), P-value in bold letters.

epidermis and the signal intensity of the dermis. In comparison to VivoSight[®], Skintell[®] has a lower signal intensity and Callisto[®] an enhanced signal intensity of the afflicted skin layers (Fig. 5b). Thus, the difference in signal intensity is even higher when comparing Callisto[®] to Skintell[®] (Fig. 5b). With Skintell[®] the measured thickness of the stratum corneum and the epidermis was lower than with VivoSight[®] and also with Callisto[®] (Fig. 5c). VivoSight[®] and Callisto[®] provided similar thickness measurement results (Fig. 5c).

Friedman's test found significant differences in the signal intensity and thickness measurements between the three OCT groups (Table 2a). The outcomes from running paired Wilcoxon tests with Bonferroni corrected *P*-values in Table 2a show significant differences in the signal intensity of AK affected skin layers between VivoSight[®] and Skintell[®] as well as between Callisto[®] and Skintell[®] measurements. Moreover there were no significant changes in the signal intensity of the epidermis and dermis, but a significant stronger signal intensity of the stratum corneum was found when comparing VivoSight[®] with Callisto[®]. Table 2b shows a significantly thicker stratum corneum and epidermis with VivoSight[®] as well as Callisto[®] measurement than Skintell[®]. Nevertheless, there were no statistically significant differences in the thickness measurement of AKs between VivoSight[®] and Callisto[®].

Comparison of three OCT systems with histology

The statistical separate analysis of the histologically confirmed subgroup, 12 BCCs of 11

TABLE 4. Statistical results of the BCC tumor thickness correlation of histology, VivoSight[®], Callisto[®] and Skintell[®] (N = 12); *r* = Spearman's correlation coefficient; the correlation is significant at a level of 0.01 (both sides)

	Histology	VivoSight [®]	Callisto [®]	Skintell [®]
Histology				
Spearman-Rho (<i>r</i>)	1.000	-0.070	-0.112	-0.196
<i>P</i> -value (both sides)	.	0.828	0.728	0.540
VivoSight [®]				
Spearman-Rho (<i>r</i>)	-0.070	1.000	0.979*	0.350
<i>P</i> -value (both sides)	0.828	.	0.000	0.265
Callisto [®]				
Spearman-Rho (<i>r</i>)	-0.112	0.979*	1.000	0.357
<i>P</i> -value (both sides)	0.728	0.000	.	0.255
Skintell [®]				
Spearman-Rho (<i>r</i>)	-0.196	0.350	0.357	1.000
<i>P</i> -value (both sides)	0.540	0.265	0.255	.

*The correlation is significant at a level of 0.01 (both sides).

patients (1 female, 10 male, median age 71.3, range 53–85 years), showed almost the same outcomes as the whole BCC study group (Table 3a and b). The only difference to the results of the whole group is that there was no significant signal intensity distinction in the dermis below the BCC between Callisto[®] and Skintell[®]. Four BCCs and eight of the 10 AKs received topical treatment. Because only two AKs were biopsied, no statistical analysis was performed but descriptive analysis was similar to the entire measured AK group.

Figure 6 represents the correlation of BCC tumor thickness measurement of VivoSight[®], Callisto[®], Skintell[®] and histology. 12 BCCs, even those with a deeper penetration than the 2 mm of OCT, took part in the correlation process. BCC tumor thickness measurements with VivoSight[®] correlated very well with Callisto[®], but less well with histology and Skintell[®] (see Table 4).

Discussion

Studies on comparison of OCT and high-frequency ultrasound, which showed a good correlation regarding thickness measurements, are available, but there is a lack of studies between different OCT devices (17, 18).

The point in comparing three OCT devices is, that the OCT systems are different depending on the chosen light source, the focus and the lens system. Due to their technical features resolution and penetration depth of the devices

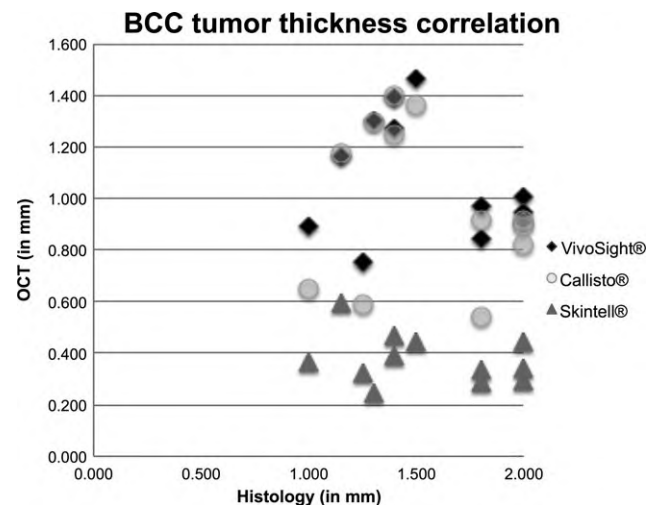


Fig. 6. The point cloud illustrates the correlation of 12 BCC tumor thickness measurements of VivoSight[®], Callisto[®], Skintell[®] and histology; thickness in mm; 2 mm = all tumors ≥ 2 mm.

vary. The time domain OCT uses an adjustable reference mirror to measure the required time for the reflection of the returning light in the depth direction (z-axis) (19). Therefore, the time domain OCT is limited in image quality and amount of data, especially in the transverse direction (19). Meanwhile the frequency or SD-OCT, which analyzes the wavelengths of the reflected light across a spectrum simultaneously because of a static reference mirror and spectrometer, enables a superior sensitivity and faster way of capturing images (3). Both time domain and spectral/frequency domain OCT use broadband light sources, whereas the swept-source OCT is based on a sweeping narrow line width laser (3).

Despite their technical differences, this study showed that all three tested OCT devices, VivoSight[®], Callisto[®] and Skintell[®], could significantly distinguish BCCs and AKs from adjacent healthy skin through signal intensity reduction and a strong thickness increase in the stratum corneum and epidermis of AKs. As demonstrated, Skintell[®] shows a lower signal intensity of all skin layers affected by BCCs and AKs as well as a thinner stratum corneum and epidermis compared to VivoSight[®] and Callisto[®]. This result could possibly depend on the higher resolution of Skintell[®], because maybe with the other two OCT devices the skin surface reflection was measured instead of or additionally to the layer thickness. It would also be conceivable, that this effect is based on the application of gel during the Skintell[®] measurement, which evokes a thinner input signal. Lastly, distance measurements have to be corrected by the refractive index of skin, which corresponds to water and is about 1.33. Possibly, the calibration factor is different between the systems.

Meanwhile, nearly all measurements between VivoSight[®] and Callisto[®] provided similar results, aside from the signal intensities of the epidermis above the BCC and of the stratum corneum in AKs. Moreover, VivoSight[®] and

Callisto[®] correlated very well regarding BCC tumor thickness, unlike with Skintell[®] and histology. The latter could be explained through the fact that only two of the 12 BCCs had a tumor size <1.2 mm, which is the often cited cut-off for OCT and histology correlation (20). Skintell[®] has a much lower detection depth of less than 700 μm compared to the other two systems, which are comparable with one another in terms of the signal penetration in skin. Therefore, Skintell[®] is inferior regarding imaging of the lower border of BCCs and determination of the infiltration depth, which is important for deciding whether a topical treatment with photodynamic therapy or imiquimod may be successful or if surgery has to be performed.

Other shortcomings of this study are that no statistical analysis of histologically confirmed AKs was performed due to the small number of surgically removed AKs. Because of the individual image selection, the inter-observer variability and due to the fact that every patient has another normal skin as control site, signal intensity and layer thickness in relation to the entire lesion could vary.

In conclusion, every OCT device is able to detect BCCs and AKs and to differentiate them from normal skin. Due to their technical specifications, differences and similarities in signal intensity and thickness measurements were noted among the three OCT systems, especially the clearly different penetration depth between Skintell[®] and the other two OCT devices was apparent. All OCT systems helped to improve the diagnostic accuracy in NMSC using objective parameters like signal intensity and thickness measurements in addition to clinical examination and dermoscopy.

Acknowledgements

Many thanks to Dipl.-Math. Karlheinz Haude for his statistical advice.

References

1. Fercher AF, Mengedoht K, Werner W. Eye-length measurement by interferometry with partially coherent light. *Opt Lett* 1988; 13: 186–188.
2. Huang D, Swanson EA, Lin CP et al. Optical coherence tomography. *Science* 1991; 254: 1178–1181.
3. Sattler EC, Kästle R, Welzel J. Optical coherence tomography in dermatology. *J Biomed Opt* 2013; 18: 061224.
4. Themstrup L, Banzhaf CA, Mogensen M, Jemec GBE. Optical coherence tomography imaging of non-melanoma skin cancer undergoing photodynamic therapy reveals sub-clinical residual lesions. *Photodiagnosis Photodyn Ther* 2014; 11: 7–12.

5. Barton JK, Gossage KW, Xu W, Ranger-Moore JR, Saboda K, Brooks CA, Duckett LD, Salasche SJ, Warneke JA, Alberts DS. Investigating sun-damaged skin and actinic keratosis with optical coherence tomography: a pilot study. *Technol Cancer Res Treat* 2003; 2: 525–535.
6. Korde VR, Bonnema GT, Xu W et al. Using optical coherence tomography to evaluate skin sun damage and precancer. *Lasers Surg Med* 2007; 39: 687–695.
7. Gambichler T, Orlikov A, Vasa R, Moussa G, Hoffmann K, Stücker M, Altmeyer P, Bechara FG. In vivo optical coherence tomography of basal cell carcinoma. *J Dermatol Sci* 2007; 45: 167–173.
8. Gao W, Zakharov VP, Myakinin OO, Bratchenko IA, Artemyev DN, Kornilin DV. Medical images classification for skin cancer using quantitative image features with optical coherence tomography. *J Innov Opt Health Sci* 2016; 9: 1650003.
9. Reifenberger J. Basalzellkarzinom. In: Plewig G and Braun-Falco O, eds. *Braun-Falco's dermatologie, venerologie und allergologie*, 6th edn. Berlin: Springer; 2012: 1633–1644.
10. Gambichler T, Plura I, Kampilafkos P, Valavanis K, Sand M, Bechara FG, Stücker M. Histopathological correlates of basal cell carcinoma in the slice and en face imaging modes of high-definition optical coherence tomography. *Br J Dermatol* 2014; 170: 1358–1361.
11. Maier T, Braun-Falco M, Laubender RP, Ruzicka T, Berking C. Actinic keratosis in the en-face and slice imaging mode of high-definition optical coherence tomography and comparison with histology. *Br J Dermatol* 2013; 168: 120–128.
12. Themstrup L, Banzhaf CA, Mogensen M, Jemec GBE. Cryosurgery treatment of actinic keratoses monitored by optical coherence tomography: a pilot study. *Dermatology (Basel)* 2012; 225: 242–247.
13. Coleman AJ, Richardson TJ, Orchard G, Uddin A, Choi MJ, Lacy KE. Histological correlates of optical coherence tomography in non-melanoma skin cancer. *Skin Res Technol* 2013; 19: 10–19.
14. Michelson Diagnostics. VivoSight OCT Scanner- Technical Specification. Available from: http://www.vivosight.com/wp-content/uploads/2013/02/1003.SP_638-Issue-1-VivoSight-Technical-Specification.pdf (accessed 18 June 2015).
15. Thorlabs GmbH. Callisto Spectral Domain OCT System: Operating Manual, 2011. Available from: <https://www.thorlabs.com/thorcat/21200/CALLISTO-Manual.pdf> (accessed 6 June 2015).
16. AGFA HealthCare. Skintell Data-sheet. Available from: <http://www.agfahealthcare.com/global/en/he/library/libraryopen?ID=34-711786> (accessed 14 September 2015).
17. Mogensen M, Nürnberg BM, Forman JL, Thomsen JB, Thrane L, Jemec GBE. In vivo thickness measurement of basal cell carcinoma and actinic keratosis with optical coherence tomography and 20-MHz ultrasound. *Br J Dermatol* 2009; 160: 1026–1033.
18. Hinz T, Ehler L, Hornung T, Voth H, Fortmeier I, Maier T, Höller T, Schmid-Wendtner MH. Preoperative characterization of basal cell carcinoma comparing tumour thickness measurement by optical coherence tomography, 20-MHz ultrasound and histopathology. *Acta Derm Venereol* 2012; 92: 132–137.
19. Wijesinghe REH, Cho NH, Park K, Shin Y, Kim J. Wavelength-filter based spectral calibrated wave number - linearization in 1.3 mm spectral domain optical coherence. *Int J Eng Adv Technol* 2013; 3: 336–340.
20. Olmedo JM, Warschaw KE, Schmitt JM, Swanson DL. Correlation of thickness of basal cell carcinoma by optical coherence tomography in vivo and routine histologic findings: a pilot study. *Dermatol Surg* 2007; 33: 421–425.

Address:

*Prof Dr Julia Welzel
 Department of Dermatology and
 Allergology
 Klinikum Augsburg
 Sauerbruchstraße 6
 D- 86179 Augsburg
 Germany
 Tel: +49 821 400 7401
 Fax: +49 821 400 17 7401
 e-mail: julia.welzel@klinikum-augsburg.de*